

Find First, Track Next: Decoupling Identification and Propagation in Referring Video Object Segmentation

Suhwan Cho^{1,*}, Seunghoon Lee^{2,*}, Minhyeok Lee², Jungho Lee², Sangyoun Lee²

¹ Independent Researcher ² Yonsei University

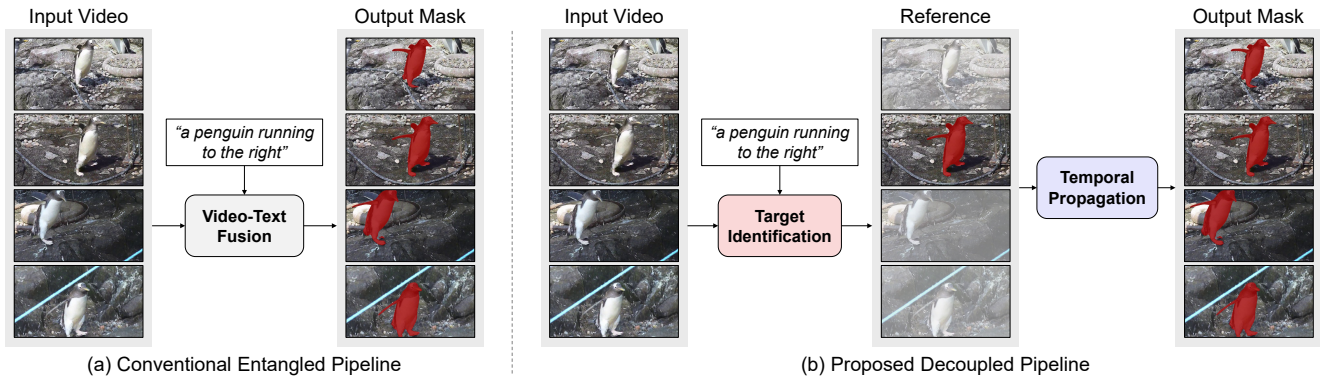


Figure 1. Visualized comparison of (a) a conventional entangled pipeline that fuses multi-modal cues in a single stage and (b) our proposed decoupled pipeline, which separates target object identification and temporal mask propagation into two distinct stages.

Abstract

Referring video object segmentation aims to segment and track a target object in a video using a natural language prompt. Existing methods typically fuse visual and textual features in a highly entangled manner, processing multi-modal information together to generate per-frame masks. However, this approach often struggles with ambiguous target identification, particularly in scenes with multiple similar objects, and fails to ensure consistent mask propagation across frames. To address these limitations, we introduce FindTrack, a novel decoupled framework that separates target identification from mask propagation. FindTrack first adaptively selects a key frame by balancing segmentation confidence and vision-text alignment, establishing a robust reference for the target object. This reference is then utilized by a dedicated propagation module to track and segment the object across the entire video. By decoupling these processes, FindTrack effectively reduces ambiguities in target association and enhances segmentation consistency. We demonstrate that FindTrack outperforms existing methods on public benchmarks. Code and models are available at <https://github.com/suhwan-cho/FindTrack>.

1. Introduction

Video object segmentation (VOS) aims to segment objects in videos and encompasses several settings. Semi-supervised VOS segments objects with an initial frame mask as guidance [6, 9, 10, 33, 39], while unsupervised VOS identifies primary objects without explicit supervision [11, 12, 20, 24, 25, 53]. Weakly-supervised VOS relies on a bounding box instead of a mask in the first frame [3, 26, 42]. In contrast, referring VOS segments an object based on a natural language prompt, requiring the model to understand both visual and textual information. This task has gained significant interest due to its applications in video editing, human-computer interaction, and multimedia analysis. However, it remains challenging due to linguistic ambiguities, occlusions, rapid motion, and appearance variations.

Existing referring VOS methods predominantly follow an entangled fusion strategy, where visual and textual features are jointly processed within a spatio-temporal framework [4, 31, 44, 50]. Typically, visual features are extracted via deep video encoders, while textual representations are obtained from language encoders. These multi-modal features are fused through attention mechanisms to generate per-frame segmentation masks. While effective, this approach has fundamental limitations. First, it often struggles

*These authors contribute equally to this work.

◊This work was done while Suhwan Cho was at Yonsei University.

with ambiguous target identification, particularly in scenes with multiple similar objects, as the model lacks an explicit reference frame to associate the language prompt with the correct object. Second, it does not enforce consistent object segmentation across frames, leading to propagation errors, especially in challenging scenarios involving occlusions, rapid motion, or appearance variations. Without a stable reference frame, existing methods fail to ensure robust and coherent mask propagation.

To address these challenges, we introduce FindTrack, a novel decoupled framework that explicitly separates object identification from mask propagation. Rather than jointly processing all frames with fused multi-modal features, FindTrack first selects a key frame adaptively by considering segmentation confidence and vision-text alignment, ensuring a reliable and unambiguous reference for the target object. This reference frame serves as a stable anchor before mask propagation begins. A dedicated propagation module then leverages this strong reference to track and segment the target object throughout the video. By decoupling these two processes, FindTrack mitigates ambiguities in object identification and enhances segmentation consistency, overcoming the limitations of entangled feature fusion in existing methods. A visual comparison between FindTrack and existing approaches is shown in Figure 1.

This decoupled framework offers several key advantages. First, by establishing a strong reference before propagation, FindTrack significantly improves target localization, reducing errors introduced by multi-modal fusion across all frames. Second, the use of a dedicated tracking mechanism ensures robust object tracking even in challenging scenarios such as occlusions and fast motion. Third, by explicitly modeling the transition from object identification to mask propagation, FindTrack provides a more structured and interpretable approach to referring VOS, offering insights that can guide future research in this domain.

Our proposed FindTrack is evaluated on three widely used referring VOS benchmarks: Ref-YouTube-VOS[38], Ref-DAVIS17[22], and MeViS [14]. Across all datasets, FindTrack achieves state-of-the-art performance, surpassing existing methods by a significant margin. Specifically, it attains a $\mathcal{J}\&\mathcal{F}$ score of 70.3% on Ref-YouTube-VOS, 74.2% on Ref-DAVIS17, and 48.2% on MeViS, demonstrating its effectiveness in various referring VOS scenarios.

Our main contributions are summarized as follows:

- We propose FindTrack, a novel framework that explicitly decouples object identification from mask propagation, overcoming the limitations of entangled fusion.
- We introduce an adaptive key frame selection strategy that leverages segmentation confidence and text alignment to establish a reliable anchor for propagation.
- FindTrack achieves state-of-the-art performance on public benchmarks, outperforming existing methods.

2. Related Work

Referring image segmentation. Referring image segmentation (RIS) focuses on segmenting the object in an image described by a natural language expression. Early methods emphasize the fusion of visual and linguistic cues. For instance, VLT [13] introduces a vision-language transformer that generates object queries by independently extracting and fusing visual and textual features, enabling robust cross-modal interaction. CRIS [43] leverages the strong image-text alignment of CLIP [37] through pixel-level contrastive learning to distinguish subtle differences between the referred object and distractors. LAVT [48] refines this fusion by integrating linguistic information at intermediate levels within the vision transformer, leading to more precise localization. Recent advances, such as GSVA [45], exploit the generalization capabilities of large-scale multi-modal models to generate effective referring prompts, while EVF-SAM [51] employs an early fusion strategy with pre-trained vision-language models to guide segmentation via elaborated prompts for SAM [23].

Referring video object segmentation. Referring VOS extends RIS to the video domain, requiring both accurate spatial segmentation and temporal consistency. Early methods focus on directly injecting text features into the visual stream. URVOS [38] introduces a unified framework that combines an image-language fusion module with a memory mechanism to ensure consistent segmentation over time, whereas CMPC-V [28] employs cross-modal attention across layers to establish fine-grained relationships between textual cues and visual features.

With the advent of DETR-based architectures [5], query-based models have significantly advanced referring VOS. MTTR [4] presents an end-to-end framework in which object-representative queries are generated and fused with multimodal features via transformers, with segmentation achieved via Hungarian matching. Building on this, RefFormer [44] leverages language as queries to interact with video features through cross-attention, further refined by a cross-modal FPN [27] decoder. SgMg [31] mitigates feature drift by incorporating Fourier domain attention with a Gaussian kernel, maintaining consistency across frames, while VD-IT [54] exploits pre-trained text-to-video diffusion models [19, 41] within a query-based matching framework that combines CLIP-generated prompts with DETR.

Recent efforts aim to better integrate linguistic cues by disentangling static attributes from dynamic features. LoSh [50] adopts a joint prediction strategy that categorizes language expressions into long and short components prior to fusion with visual features, and DsHmp [18] introduces a hierarchical perception module that decomposes language into static and motion parts while segmenting the target object into multiple regions for fine-grained alignment.

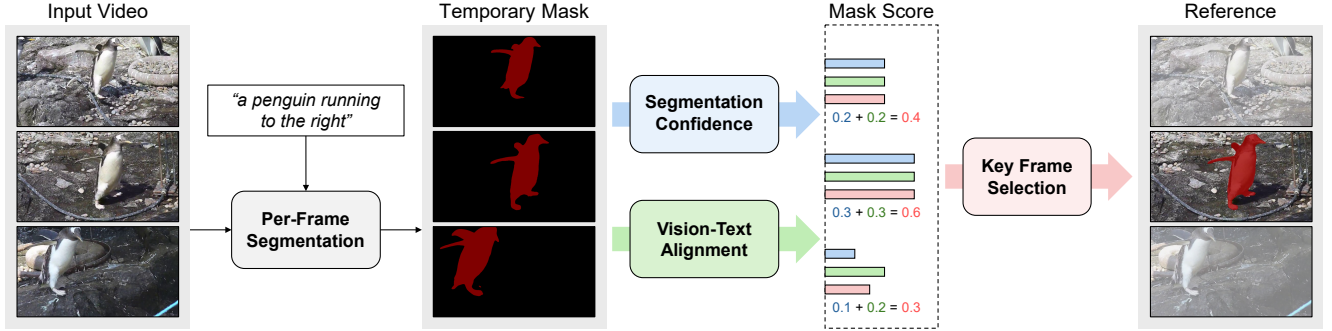


Figure 2. Visual representation of the target object identification process, the first step of FindTrack. Given an input video, candidate key frames are sampled to evaluate frame-level segmentation quality. The key frame is then selected based on segmentation confidence and vision-text alignment, serving as a reference for the next step.

Despite these advancements, existing methods still face challenges. Entangled fusion strategies, which process visual and textual features jointly across all frames, can lead to ambiguous target identification in scenes with similar objects. Moreover, without a stable reference for segmentation, these approaches often suffer from propagation errors under occlusions or fast motion. Our work, FindTrack, addresses these limitations by explicitly decoupling object identification from mask propagation, thereby establishing a reliable reference and ensuring stable tracking of the target object across frames.

3. Approach

3.1. Problem Formulation

The objective of referring VOS is to segment the target object specified by a given language expression across all frames of a video. Formally, let the input video frames be denoted as $I := \{I^1, I^2, \dots, I^T\}$, where T is the total number of frames. The corresponding ground truth binary masks are represented as $M := \{M^1, M^2, \dots, M^T\}$, and the language expression describing the target object is given by L . The goal is to predict a sequence of segmentation masks, $\hat{M} := \{\hat{M}^1, \hat{M}^2, \dots, \hat{M}^T\}$, that accurately localizes the referred object in each frame based on I and L .

3.2. System Overview

Existing methods fuse visual and textual features in a single-stage manner, as shown in Figure 1 (a), often leading to ambiguous target identification and inconsistent object tracking. To overcome these limitations, we propose a decoupled pipeline that explicitly separates target identification from temporal propagation, as illustrated in Figure 1 (b). Given video frames and a language expression, our approach first selects a key frame and predicts its segmentation mask. This mask is then bi-directionally propagated across the entire video, ensuring robust and consistent tracking of the target object specified by the text input.

3.3. Target Identification

The objective of target identification is to determine the target object specified by the language prompt within a video. This step focuses on localizing the most confident object in a single frame, rather than predicting the object mask across all frames, as the designated object will be tracked in the subsequent step. A visual representation of the target identification pipeline is shown in Figure 2.

Per-frame segmentation. To localize the target object with the highest confidence, we scan the video frames and predict the segmentation mask based on the language prompt. However, processing all frames incurs significant computational costs. To address this, we first sample candidate key frames and perform per-frame segmentation on them. The candidate key frames are defined as $C := \{j\}_{i=1}^N$ where

$$j = \lfloor \frac{(i-1) * (T-1)}{N-1} \rfloor + 1, \quad (1)$$

and N denotes the total number of sampled frames. For the uniformly sampled candidate key frames C , we apply a per-frame segmentation model, EVF-SAM [51], resulting in a temporary mask set \tilde{M} and the corresponding segmentation confidence π :

$$\tilde{M}, \pi := \{\Psi(I^j, L)\}_{i=1}^N, \quad (2)$$

where Ψ represents the per-frame referring segmentation model. The frame indices j are determined as per Eqn.1.

Key frame selection. From the temporary mask set \tilde{M} , we select the most reliable prediction as the key frame, which serves as a strong reference for target object tracking. The quality of each segmentation mask is assessed based on two criteria: 1) the segmentation confidence of the predicted mask and 2) the vision-text alignment between the visual content within the mask and the input language expression.

Segmentation confidence π represents the predicted intersection over union (IoU) score of the generated mask.

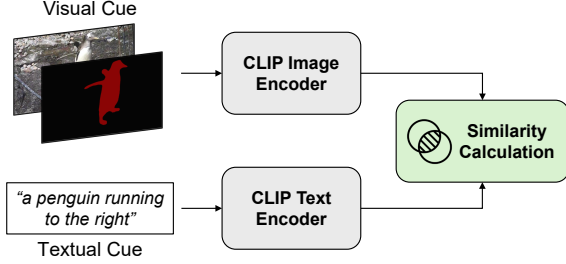


Figure 3. Visualized pipeline of the vision-text alignment stage. The similarity between the pixels within the predicted mask and the given text is evaluated to ensure contextual alignment.

This confidence is learned alongside mask prediction during the training of the referring segmentation model. A high segmentation confidence suggests that the mask is likely to have a high IoU with the ground truth, thereby increasing the likelihood that the selected key frame will serve as an effective reference during temporal propagation. This confidence is directly derived from the segmentation decoder, as indicated in Eqn. 2, which we employ as our per-frame referring segmentation model.

However, in some cases, even a high-confidence mask may fail to accurately localize the object with respect to the language prompt. To address this, we employ Alpha-CLIP [40] to estimate the vision-text alignment score, ensuring that the selected key frame is not only reliable in segmentation but also well-aligned with the text prompt:

$$\rho = \mathcal{N}(\text{CLIP}_{img}(I \oplus \tilde{M})) \cdot \mathcal{N}(\text{CLIP}_{text}), \quad (3)$$

where CLIP_{img} and CLIP_{text} denote the image and text encoders of Alpha-CLIP, respectively, and \mathcal{N} represents L2 normalization along the channel dimension. By computing the cosine similarity between the visual and textual embeddings, we assess how well the visual content within the predicted mask aligns with the textual description. This allows us to verify whether the target object is correctly localized. This process is also visualized in Figure 3. Finally, the overall mask score for each frame σ is computed as

$$\sigma = w_1\pi + w_2\rho, \quad (4)$$

where w_1 and w_2 denotes the weighting factor for the segmentation confidence score and vision-text alignment score, respectively. The final mask score serves as the criterion for key frame selection, defined as

$$k = \{\arg \max_j \sigma^j\}_{i=1}^N, \quad (5)$$

where k represents the key frame used as a reference for temporal propagation.

3.4. Temporal Propagation

In the temporal mask propagation stage, the key frame selected in the previous step serves as a reference for prop-

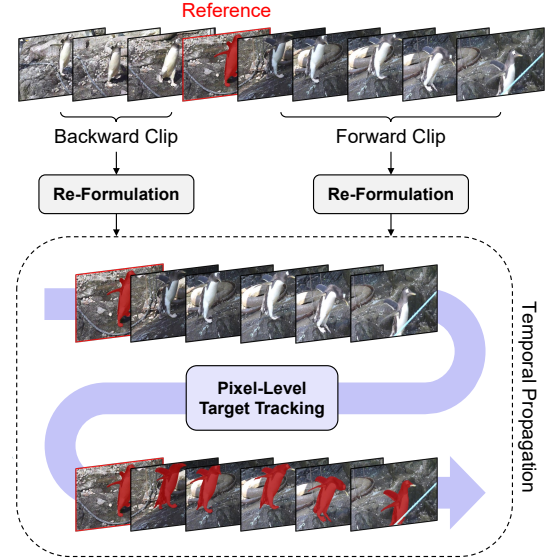


Figure 4. Visualized pipeline of temporal mask propagation. The video is split into two clips at the key frame, with each clip processed by the pixel-level tracking network.

agating the target object’s mask across subsequent video frames. This propagation exploits the temporal coherence of the object and the visual context in adjacent frames to ensure accurate localization throughout the sequence. The core idea is to transfer the target object’s mask from the key frame while preserving consistency. To achieve this, we utilize the architecture of Cutie [8]. The overall pipeline for temporal propagation is visualized in Figure 4.

Sequence re-formulation. Unlike existing approaches that directly detect the target object without an explicit visual reference, we track the object using a strong reference, specifically the predicted mask at the key frame. To exploit the visual prior of the target object, we first split the video into two clips:

$$I_{fw} := \{I^k, I^{k+1}, \dots, I^T\} \quad (6)$$

$$I_{bw} := \{I^k, I^{k-1}, \dots, I^1\}, \quad (7)$$

where I_{fw} and I_{bw} denote the forward and backward video clips, respectively. The first frame in each clip is initialized with the segmentation mask, providing strong guidance for tracking the target object.

Pixel-level tracking. To achieve precise mask propagation, we employ a memory-based pixel tracking network [6–8, 33], as detailed in Algorithm 1. This architecture, commonly used in semi-supervised VOS, maintains a dynamic memory bank that continuously stores and retrieves object features, ensuring accurate and temporally consistent segmentation throughout the video. By leveraging memory-based tracking, our approach effectively handles challenges

Algorithm 1 Pixel-Level Tracking

```
1: Input:  $I, \tilde{M}^k$ 
2: Output:  $\hat{M}$ 
3: Initialize  $\hat{M}^k$  with  $\tilde{M}^k$ 
4: Initialize memory with  $(I^k, \tilde{M}^k)$ 
5: for each frame  $t$  in  $\{k+1, k+2, \dots, T\}$  do
6:   Predict  $\hat{M}^t$  using  $I^t$  and memory
7:   Update memory with  $(I^t, \hat{M}^t)$ 
8: end for
9: Initialize memory with  $(I^k, \tilde{M}^k)$ 
10: for each frame  $t$  in  $\{k-1, k-2, \dots, 1\}$  do
11:   Predict  $\hat{M}^t$  using  $I^t$  and memory
12:   Update memory with  $(I^t, \hat{M}^t)$ 
13: end for
```

such as object deformation and occlusions, which often degrade segmentation performance in dynamic scenes.

The process begins by initializing the memory with the key frame image I^k and its predicted mask \tilde{M}^k . The memory module captures rich visual embeddings of the target object, which are then retrieved to guide mask prediction in subsequent frames. Propagation follows a bi-directional strategy, where the forward clip I_{fw} and backward clip I_{bw} are processed independently. At each step, the model predicts the segmentation mask for the current frame based on stored memory representations and updates the memory with the newly processed frame and its mask. This iterative update mechanism enhances robustness to appearance changes and complex motion patterns, ensuring stable mask propagation even in challenging scenarios with background clutter or fast-moving objects.

By structuring mask propagation within a memory-based tracking framework, our approach reliably transfers the key frame mask across the entire video sequence. The model continuously refines segmentation accuracy by leveraging both spatial and temporal cues accumulated over time. As a result, we obtain the final segmentation mask prediction \hat{M} , providing temporally coherent and spatially precise object tracking across all frames.

3.5. Implementation Details

Model setup. FindTrack consists of three core networks: EVF-SAM [51], Alpha-CLIP [40], and Cutie [8]. EVF-SAM uses a BEiT [2] backbone to provide language guidance for the SAM [23] decoder. It is trained on standard RIS datasets, including the RefCOCO variants [21, 30, 32, 49], ADE20K [52], and others. Alpha-CLIP is trained on GRIT-20M [34] using RGBA region-text pairs. Cutie is trained under the MEGA setting, which integrates several VOS datasets [1, 15, 35, 36, 46]. Notably, our system requires no additional training, as the roles of each component are effectively decoupled and seamlessly integrated to fully leverage the knowledge gained from each task.

Inference setup. In the target identification stage, we uniformly sample N frames from the video sequence as candidate key frames for temporal propagation, setting $N = 5$ by default to balance performance and inference speed. The mask score σ for each candidate frame is computed as a weighted sum of the segmentation confidence score π and the vision-text alignment score ρ , with weights $w_1 = 0.5$ and $w_2 = 0.5$. The frame with the highest mask score is selected as the key frame. For temporal propagation, memory in the tracking model is updated every three frames, with long-term memory extraction disabled by default.

We maintain a consistent inference setup across all benchmarks, including candidate frame sampling, key frame selection criteria, and memory update policy. Two exceptions apply: 1) on Ref-YouTube-VOS [38], where frames are provided at five-frame intervals, memory is updated accordingly; 2) on MeViS [14], which contains extremely long videos, long-term memory is enabled. While this standardized setup ensures generalizability, further tuning may improve performance.

Our model runs on a single GeForce RTX 3090 GPU. Under the representative setting, processing a 30-frame video clip requires approximately 7.9 GB of GPU memory, with an inference speed of around 10 fps.

4. Experiments

4.1. Datasets

We evaluate FindTrack on three established referring VOS benchmarks: Ref-YouTube-VOS [38], Ref-DAVIS17 [22], and MeViS [14]. Ref-YouTube-VOS extends YouTube-VOS [46] with referring annotations, providing 202 validation videos. Ref-DAVIS17 is built on DAVIS [35], comprising 30 videos, where each object is annotated with four language expressions. MeViS [14] is a large-scale dataset designed for motion-aware referring segmentation, featuring 140 validation videos and 2,236 language expressions.

4.2. Evaluation Metrics

We evaluate performance using three standard metrics: region similarity (\mathcal{J}), boundary accuracy (\mathcal{F}), and their average ($\mathcal{J}\&\mathcal{F}$). The \mathcal{J} and \mathcal{F} scores are computed as follows:

$$\mathcal{J} = \frac{|M_{gt} \cap M_{pred}|}{|M_{gt} \cup M_{pred}|}, \quad (8)$$

$$\mathcal{F} = \frac{2 \times \text{Precision} \times \text{Recall}}{\text{Precision} + \text{Recall}}. \quad (9)$$

4.3. Qualitative Results

In Figure 5, we compare FindTrack with state-of-the-art methods, SgMg [31] and MUTR [47], on the Ref-YouTube-VOS [38] dataset. The first example illustrates a case where

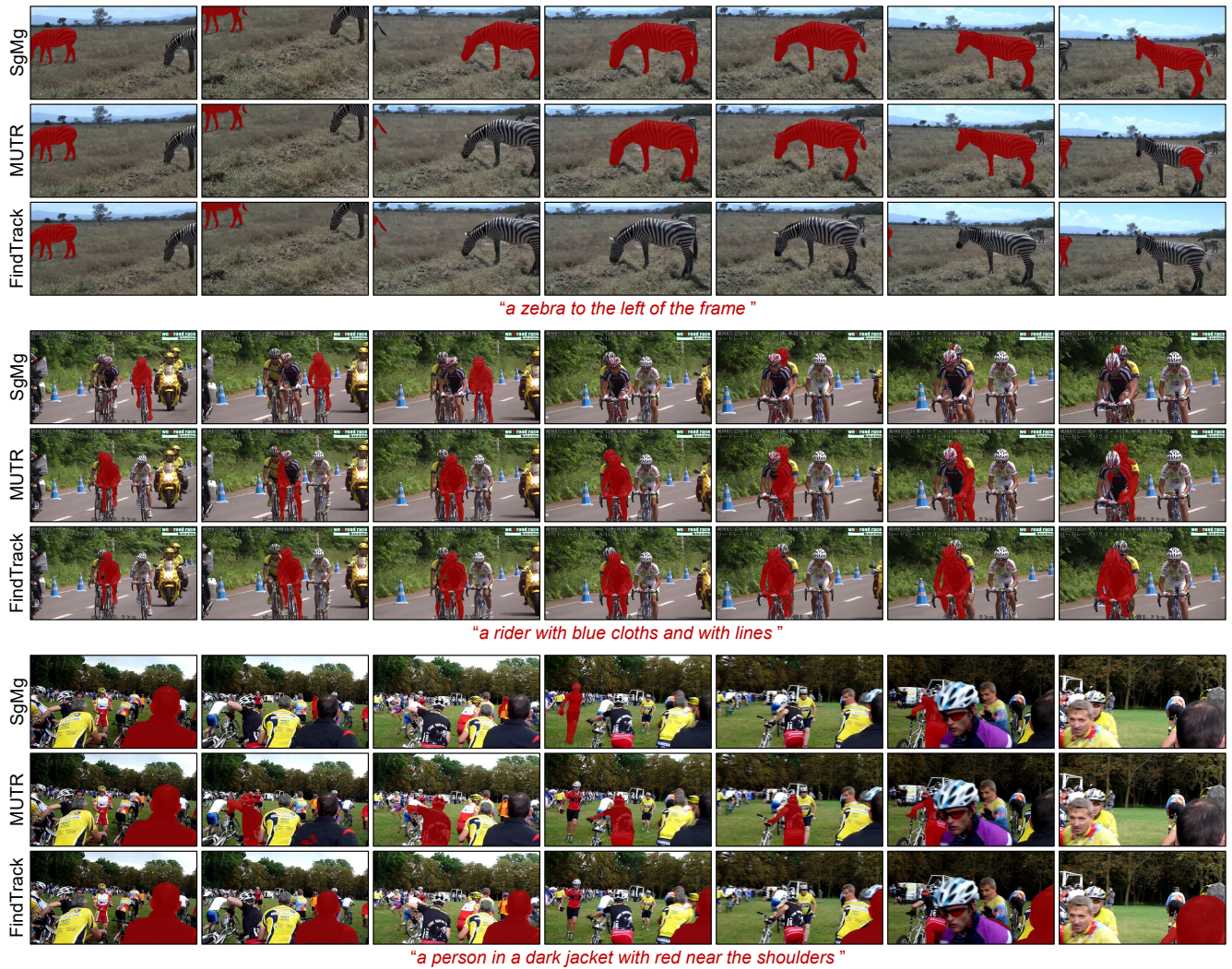


Figure 5. Qualitative comparison between FindTrack and state-of-the-art methods.

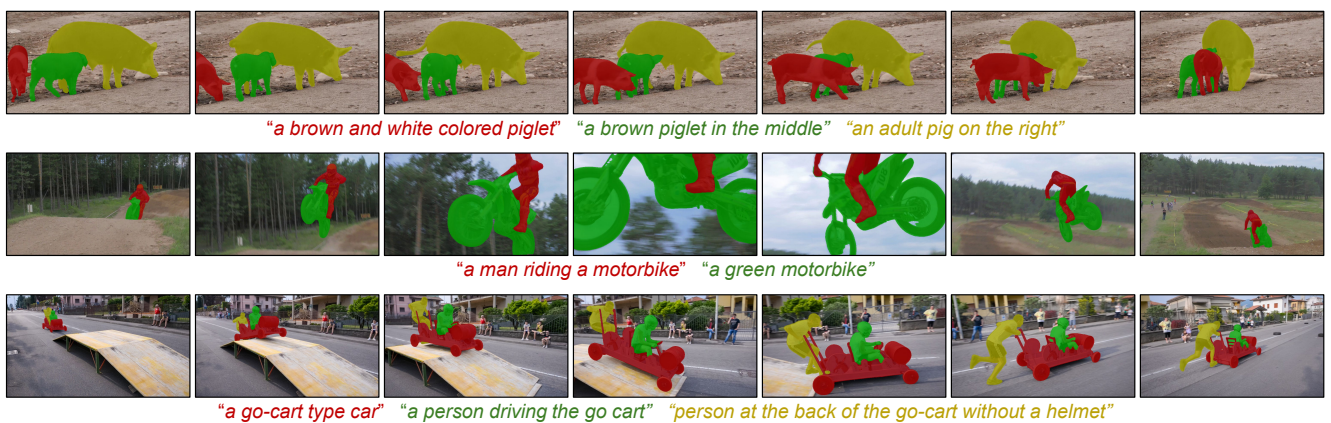


Figure 6. Qualitative results of FindTrack in challenging scenarios.

the target object exits the frame due to significant camera movement, with visually similar objects appearing in subsequent frames. The second and third examples depict sce-

narios where the target object becomes entangled with challenging visual distractors. In both cases, SgMg and MUTR struggle to correctly identify the target, as they fail to ef-

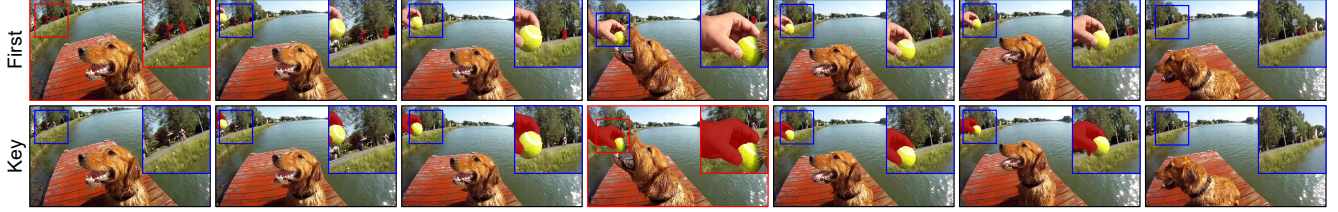


Figure 7. Visualization of results from different reference selection protocols, with the reference highlighted in red.

Table 1. Quantitative evaluation on the Ref-YouTube-VOS validation set, Ref-DAVIS17 dataset, and MeViS validation set.

Method	Publication	Ref-YouTube-VOS			Ref-DAVIS17			MeViS		
		$\mathcal{J}\&\mathcal{F}$	\mathcal{J}	\mathcal{F}	$\mathcal{J}\&\mathcal{F}$	\mathcal{J}	\mathcal{F}	$\mathcal{J}\&\mathcal{F}$	\mathcal{J}	\mathcal{F}
URVOS [38]	ECCV'20	47.2	45.3	49.2	51.6	47.3	56.0	27.8	25.7	29.9
LBDT [16]	CVPR'22	49.4	48.2	50.6	54.5	-	-	29.3	27.8	30.8
ReferFormer [44]	CVPR'22	62.9	61.3	64.6	61.1	58.1	64.1	31.0	29.8	32.2
MTTR [4]	CVPR'22	55.3	54.0	56.6	-	-	-	30.0	28.8	31.2
SgMg [31]	ICCV'23	65.7	63.9	67.4	63.3	60.6	66.0	-	-	-
HTML [17]	ICCV'23	63.4	61.5	65.2	62.1	59.2	65.1	-	-	-
SOC [29]	NeurIPS'23	67.3	65.3	69.3	65.8	62.5	69.1	-	-	-
VLt+TC [13]	TPAMI'23	62.7	-	-	60.3	-	-	35.5	33.6	37.3
MUTR [47]	AAAI'24	68.4	66.4	70.4	68.0	64.8	71.3	-	-	-
LoSh [50]	CVPR'24	67.2	65.4	69.0	64.3	61.8	66.8	-	-	-
DsHmp [18]	CVPR'24	67.1	65.0	69.1	64.9	61.7	68.1	46.4	43.0	49.8
VD-IT [54]	ECCV'24	66.5	64.4	68.5	69.4	66.2	72.6	-	-	-
FindTrack ($N = 5$)		70.3	68.6	72.0	74.2	69.9	78.5	47.0	44.3	49.7
FindTrack ($N = 10$)		70.3	68.6	71.9	73.7	69.4	78.0	48.2	45.6	50.7

fectively leverage temporal continuity, making them susceptible to confusion with similar-looking objects. In contrast, FindTrack constructs a robust reference from a global temporal perspective, enabling accurate target identification and consistent mask propagation throughout the video.

Figure 6 presents qualitative results of FindTrack on the Ref-DAVIS17 [22] dataset, demonstrating its robustness in complex scenarios involving multiple entangled objects, large camera movements, and background clutter, which can significantly degrade the performance of existing methods. FindTrack maintains consistent segmentation quality across these challenging conditions, highlighting its resilience to scene complexity.

4.4. Quantitative Results

In Table 1, we compare the performance of FindTrack with state-of-the-art methods on the Ref-YouTube-VOS [38], Ref-DAVIS17 [22], and MeViS [14] datasets. With the default setting of $N = 5$, FindTrack outperforms all existing methods, achieving improvements of 1.9%, 6.2%, and 0.6% on these datasets, respectively. On the MeViS validation set, which contains long video sequences resulting in sparse reference searching, increasing N to 10 provides an additional 1.0% performance gain by increasing the density of candidate frame sampling during the target identification stage.

Table 2. Ablation study on reference selection.

Reference	$\mathcal{J}\&\mathcal{F}$	\mathcal{J}	\mathcal{F}
First Frame	65.3	63.4	67.2
Last Frame	60.5	59.0	62.0
Random Frame	65.4	63.6	67.2
Key Frame	70.3	68.6	72.0

4.5. Analysis

Reference selection. Defining an effective reference for temporal propagation is crucial, as it forms the basis for target object segmentation throughout the video. To evaluate the impact of different reference selection strategies, we compare several protocols in Table 2 on the Ref-YouTube-VOS [38] validation set. First Frame simulates the direct integration of an RIS network with a semi-supervised VOS network, while Last Frame and Random Frame serve as variations of this approach. Key Frame refers to the frame selected using our candidate search strategy. The results demonstrate that selecting a reference from a temporally global perspective improves the reliability of per-frame predictions, leading to enhanced video performance.

Figure 7 presents a visual comparison between using the first frame as a reference and our proposed key frame



Figure 8. Visualization of candidate key frames with their corresponding scores, along with the final results using different mask score calculation protocols. The scores are color-coded in accordance with Figure 2, with the reference frame highlighted in red.

Table 3. Ablation study on the mask score weights.

w_1	w_2	$\mathcal{J} \& \mathcal{F}$	\mathcal{J}	\mathcal{F}
1.0	0.0	69.9	68.2	71.7
0.8	0.2	70.0	68.3	71.7
0.5	0.5	70.3	68.6	72.0
0.2	0.8	69.7	68.0	71.6
0.0	1.0	67.3	65.4	69.1

strategy. Since the target object, identified by the language prompt, does not appear early in the video, using the first frame as a reference fails to provide a reliable cue for object identification, instead capturing an incorrect cue that identifies a different object. Consistent with the quantitative analysis, segmentation quality varies significantly based on the visual characteristics of the frame, highlighting the importance of reference selection.

Mask score derivation. Reference selection among candidate key frames is based on two key criteria: segmentation confidence and vision-text alignment scores. The final reference is determined using a weighted sum of these scores. Table 3 compares the performance of different mask score weightings on the Ref-YouTube-VOS validation set. The results indicate that combining both metrics leads to better performance than using either score alone, as they effectively complement each other. Empirically, we find that setting w_1 and w_2 to 0.5 yields the best results.

Additionally, Figure 8 qualitatively demonstrates the effectiveness of our mask score derivation protocol. The first row presents candidate key frames along with their segmentation confidence and vision-text alignment scores. When only the segmentation confidence score is used (second row), incorrectly segmented frames may be selected as references, leading to error propagation. In contrast, incorporating the vision-text alignment score (third row) helps filter out inaccurate masks by assessing their consistency with the language prompt, resulting in more reliable reference selection and improved segmentation quality.

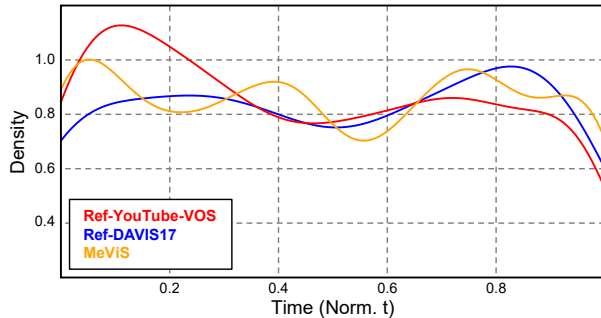


Figure 9. Visualization of key frame locations.

Key frame distribution. To further validate our reference selection protocol, we visualize the sampled key frame locations in Figure 9 using kernel density estimation. The key frames are quite evenly distributed throughout the video, indicating that the reference selection process is both unbiased and well-balanced.

Limitations. In FindTrack, the accuracy of the target object detected in the reference is critical to the final result. Consequently, any misidentification of the object during the initial stage can lead to inevitable errors in subsequent frames. This limitation can be addressed by incorporating a plug-and-play replacement with a more advanced identifier, as FindTrack’s fully modular and independent components offer a vertical solution, enabling seamless improvements.

5. Conclusion

We present FindTrack, a groundbreaking approach for referring VOS that decisively decouples target identification from temporal propagation, outperforming all existing methods on public benchmark datasets. By setting a new standard in referring VOS, FindTrack lays a robust foundation for future advancements and innovations in the field.

References

- [1] Ali Athar, Jonathon Luiten, Paul Voigtlaender, Tarasha Khurana, Achal Dave, Bastian Leibe, and Deva Ramanan. Burst: A benchmark for unifying object recognition, segmentation and tracking in video. In *Proceedings of the IEEE/CVF winter conference on applications of computer vision*, pages 1674–1683, 2023. [v](#)
- [2] Hangbo Bao, Li Dong, Songhao Piao, and Furu Wei. Beit: Bert pre-training of image transformers. *arXiv preprint arXiv:2106.08254*, 2021. [v](#)
- [3] Goutam Bhat, Felix Järemo Lawin, Martin Danelljan, Andreas Robinson, Michael Felsberg, Luc Van Gool, and Radu Timofte. Learning what to learn for video object segmentation. In *Computer Vision—ECCV 2020: 16th European Conference, Glasgow, UK, August 23–28, 2020, Proceedings, Part II 16*, pages 777–794. Springer, 2020. [i](#)
- [4] Adam Botach, Evgenii Zheltonozhskii, and Chaim Baskin. End-to-end referring video object segmentation with multimodal transformers. In *Proceedings of the IEEE/CVF Conference on Computer Vision and Pattern Recognition*, pages 4985–4995, 2022. [i](#), [ii](#), [vii](#)
- [5] Nicolas Carion, Francisco Massa, Gabriel Synnaeve, Nicolas Usunier, Alexander Kirillov, and Sergey Zagoruyko. End-to-end object detection with transformers. In *European conference on computer vision*, pages 213–229. Springer, 2020. [ii](#)
- [6] Ho Kei Cheng and Alexander G Schwing. Xmem: Long-term video object segmentation with an atkinson-shiffrin memory model. In *European Conference on Computer Vision*, pages 640–658. Springer, 2022. [i](#), [iv](#)
- [7] Ho Kei Cheng, Yu-Wing Tai, and Chi-Keung Tang. Rethinking space-time networks with improved memory coverage for efficient video object segmentation. *Advances in neural information processing systems*, 34:11781–11794, 2021.
- [8] Ho Kei Cheng, Seoung Wug Oh, Brian Price, Joon-Young Lee, and Alexander Schwing. Putting the object back into video object segmentation. In *Proceedings of the IEEE/CVF Conference on Computer Vision and Pattern Recognition*, pages 3151–3161, 2024. [iv](#), [v](#)
- [9] Suhwan Cho, Heansung Lee, Minjung Kim, Sungjun Jang, and Sangyoun Lee. Pixel-level bijective matching for video object segmentation. In *Proceedings of the IEEE/CVF Winter Conference on Applications of Computer Vision*, pages 129–138, 2022. [i](#)
- [10] Suhwan Cho, Heansung Lee, Minhyeok Lee, Chaewon Park, Sungjun Jang, Minjung Kim, and Sangyoun Lee. Tackling background distraction in video object segmentation. In *European Conference on Computer Vision*, pages 446–462. Springer, 2022. [i](#)
- [11] Suhwan Cho, Minhyeok Lee, Seunghoon Lee, Chaewon Park, Donghyeong Kim, and Sangyoun Lee. Treating motion as option to reduce motion dependency in unsupervised video object segmentation. In *Proceedings of the IEEE/CVF winter conference on applications of computer vision*, pages 5140–5149, 2023. [i](#)
- [12] Suhwan Cho, Minhyeok Lee, Seunghoon Lee, Dogyoon Lee, Heeseung Choi, Ig-Jae Kim, and Sangyoun Lee. Dual prototype attention for unsupervised video object segmentation. In *Proceedings of the IEEE/CVF Conference on Computer Vision and Pattern Recognition*, pages 19238–19247, 2024. [i](#)
- [13] Henghui Ding, Chang Liu, Suchen Wang, and Xudong Jiang. Vision-language transformer and query generation for referring segmentation. In *Proceedings of the IEEE/CVF International Conference on Computer Vision*, pages 16321–16330, 2021. [ii](#), [vii](#)
- [14] Henghui Ding, Chang Liu, Shuting He, Xudong Jiang, and Chen Change Loy. Mevis: A large-scale benchmark for video segmentation with motion expressions. In *Proceedings of the IEEE/CVF International Conference on Computer Vision*, pages 2694–2703, 2023. [ii](#), [v](#), [vii](#)
- [15] Henghui Ding, Chang Liu, Shuting He, Xudong Jiang, Philip HS Torr, and Song Bai. Mose: A new dataset for video object segmentation in complex scenes. In *Proceedings of the IEEE/CVF international conference on computer vision*, pages 20224–20234, 2023. [v](#)
- [16] Zihan Ding, Tianrui Hui, Junshi Huang, Xiaoming Wei, Jizhong Han, and Si Liu. Language-bridged spatial-temporal interaction for referring video object segmentation. In *Proceedings of the IEEE/CVF Conference on Computer Vision and Pattern Recognition*, pages 4964–4973, 2022. [vii](#)
- [17] Mingfei Han, Yali Wang, Zhihui Li, Lina Yao, Xiaojun Chang, and Yu Qiao. Htm: Hybrid temporal-scale multimodal learning framework for referring video object segmentation. In *Proceedings of the IEEE/CVF International Conference on Computer Vision*, pages 13414–13423, 2023. [vii](#)
- [18] Shuting He and Henghui Ding. Decoupling static and hierarchical motion perception for referring video segmentation. In *Proceedings of the IEEE/CVF Conference on Computer Vision and Pattern Recognition*, pages 13332–13341, 2024. [ii](#), [vii](#)
- [19] Jonathan Ho, Tim Salimans, Alexey Gritsenko, William Chan, Mohammad Norouzi, and David J Fleet. Video diffusion models. *Advances in Neural Information Processing Systems*, 35:8633–8646, 2022. [ii](#)
- [20] Ge-Peng Ji, Keren Fu, Zhe Wu, Deng-Ping Fan, Jianbing Shen, and Ling Shao. Full-duplex strategy for video object segmentation. In *Proceedings of the IEEE/CVF international conference on computer vision*, pages 4922–4933, 2021. [i](#)
- [21] Sahar Kazemzadeh, Vicente Ordonez, Mark Matten, and Tamara Berg. Referitgame: Referring to objects in photographs of natural scenes. In *Proceedings of the 2014 conference on empirical methods in natural language processing (EMNLP)*, pages 787–798, 2014. [v](#)
- [22] Anna Khoreva, Anna Rohrbach, and Bernt Schiele. Video object segmentation with language referring expressions. In *Computer Vision—ACCV 2018: 14th Asian Conference on Computer Vision, Perth, Australia, December 2–6, 2018, Revised Selected Papers, Part IV 14*, pages 123–141. Springer, 2019. [ii](#), [v](#), [vii](#)
- [23] Alexander Kirillov, Eric Mintun, Nikhila Ravi, Hanzi Mao, Chloe Rolland, Laura Gustafson, Tete Xiao, Spencer Whitehead, Alexander C Berg, Wan-Yen Lo, et al. Segment anything. In *Proceedings of the IEEE/CVF international conference on computer vision*, pages 4015–4026, 2023. [ii](#), [v](#)

- [24] Minhyeok Lee, Suhwan Cho, Seunghoon Lee, Chaewon Park, and Sangyoun Lee. Unsupervised video object segmentation via prototype memory network. In *Proceedings of the IEEE/CVF winter conference on applications of computer vision*, pages 5924–5934, 2023. [i](#)
- [25] Minhyeok Lee, Suhwan Cho, Dogyoon Lee, Chaewon Park, Jungho Lee, and Sangyoun Lee. Guided slot attention for unsupervised video object segmentation. In *Proceedings of the IEEE/CVF Conference on Computer Vision and Pattern Recognition*, pages 3807–3816, 2024. [i](#)
- [26] Fanchao Lin, Hongtao Xie, Yan Li, and Yongdong Zhang. Query-memory re-aggregation for weakly-supervised video object segmentation. In *Proceedings of the AAAI conference on artificial intelligence*, pages 2038–2046, 2021. [i](#)
- [27] Tsung-Yi Lin, Piotr Dollár, Ross Girshick, Kaiming He, Bharath Hariharan, and Serge Belongie. Feature pyramid networks for object detection. In *Proceedings of the IEEE conference on computer vision and pattern recognition*, pages 2117–2125, 2017. [ii](#)
- [28] Si Liu, Tianrui Hui, Shaofei Huang, Yunchao Wei, Bo Li, and Guanbin Li. Cross-modal progressive comprehension for referring segmentation. *IEEE Transactions on Pattern Analysis and Machine Intelligence*, 44(9):4761–4775, 2021. [ii](#)
- [29] Zhuoyan Luo, Yicheng Xiao, Yong Liu, Shuyan Li, Yitong Wang, Yansong Tang, Xiu Li, and Yujiu Yang. Soc: Semantic-assisted object cluster for referring video object segmentation. *Advances in Neural Information Processing Systems*, 36:26425–26437, 2023. [viii](#)
- [30] Junhua Mao, Jonathan Huang, Alexander Toshev, Oana Camburu, Alan L Yuille, and Kevin Murphy. Generation and comprehension of unambiguous object descriptions. In *Proceedings of the IEEE conference on computer vision and pattern recognition*, pages 11–20, 2016. [v](#)
- [31] Bo Miao, Mohammed Bennamoun, Yongsheng Gao, and Ajmal Mian. Spectrum-guided multi-granularity referring video object segmentation. In *Proceedings of the IEEE/CVF International Conference on Computer Vision*, pages 920–930, 2023. [i](#), [ii](#), [v](#), [vii](#)
- [32] Varun K Nagaraja, Vlad I Morariu, and Larry S Davis. Modeling context between objects for referring expression understanding. In *Computer Vision–ECCV 2016: 14th European Conference, Amsterdam, The Netherlands, October 11–14, 2016, Proceedings, Part IV 14*, pages 792–807. Springer, 2016. [v](#)
- [33] Seoung Wug Oh, Joon-Young Lee, Ning Xu, and Seon Joo Kim. Video object segmentation using space-time memory networks. In *Proceedings of the IEEE/CVF international conference on computer vision*, pages 9226–9235, 2019. [i](#), [iv](#)
- [34] Zhiliang Peng, Wenhui Wang, Li Dong, Yaru Hao, Shaohan Huang, Shuming Ma, and Furu Wei. Kosmos-2: Grounding multimodal large language models to the world. *arXiv preprint arXiv:2306.14824*, 2023. [v](#)
- [35] Federico Perazzi, Jordi Pont-Tuset, Brian McWilliams, Luc Van Gool, Markus Gross, and Alexander Sorkine-Hornung. A benchmark dataset and evaluation methodology for video object segmentation. In *Proceedings of the IEEE conference on computer vision and pattern recognition*, pages 724–732, 2016. [v](#)
- [36] Jiyang Qi, Yan Gao, Yao Hu, Xinggang Wang, Xiaoyu Liu, Xiang Bai, Serge Belongie, Alan Yuille, Philip HS Torr, and Song Bai. Occluded video instance segmentation: A benchmark. *International Journal of Computer Vision*, 130(8): 2022–2039, 2022. [v](#)
- [37] Alec Radford, Jong Wook Kim, Chris Hallacy, Aditya Ramesh, Gabriel Goh, Sandhini Agarwal, Girish Sastry, Amanda Askell, Pamela Mishkin, Jack Clark, et al. Learning transferable visual models from natural language supervision. In *International conference on machine learning*, pages 8748–8763. Pmlr, 2021. [ii](#)
- [38] Seonguk Seo, Joon-Young Lee, and Bohyung Han. Urvos: Unified referring video object segmentation network with a large-scale benchmark. In *Computer Vision–ECCV 2020: 16th European Conference, Glasgow, UK, August 23–28, 2020, Proceedings, Part XV 16*, pages 208–223. Springer, 2020. [ii](#), [v](#), [vii](#)
- [39] Hongje Seong, Junhyuk Hyun, and Euntai Kim. Kernelized memory network for video object segmentation. In *Computer Vision–ECCV 2020: 16th European Conference, Glasgow, UK, August 23–28, 2020, Proceedings, Part XXII 16*, pages 629–645. Springer, 2020. [i](#)
- [40] Zeyi Sun, Ye Fang, Tong Wu, Pan Zhang, Yuhang Zang, Shu Kong, Yuanjun Xiong, Dahua Lin, and Jiaqi Wang. Alpha-clip: A clip model focusing on wherever you want. In *Proceedings of the IEEE/CVF conference on computer vision and pattern recognition*, pages 13019–13029, 2024. [iv](#), [v](#)
- [41] Jiuniu Wang, Hangjie Yuan, Dayou Chen, Yingya Zhang, Xiang Wang, and Shiwei Zhang. Modelscope text-to-video technical report. *arXiv preprint arXiv:2308.06571*, 2023. [ii](#)
- [42] Qiang Wang, Li Zhang, Luca Bertinetto, Weiming Hu, and Philip HS Torr. Fast online object tracking and segmentation: A unifying approach. In *Proceedings of the IEEE/CVF conference on Computer Vision and Pattern Recognition*, pages 1328–1338, 2019. [i](#)
- [43] Zhaoqing Wang, Yu Lu, Qiang Li, Xunqiang Tao, Yandong Guo, Mingming Gong, and Tongliang Liu. Cris: Clip-driven referring image segmentation. In *Proceedings of the IEEE/CVF conference on computer vision and pattern recognition*, pages 11686–11695, 2022. [ii](#)
- [44] Jiannan Wu, Yi Jiang, Peize Sun, Zehuan Yuan, and Ping Luo. Language as queries for referring video object segmentation. In *Proceedings of the IEEE/CVF Conference on Computer Vision and Pattern Recognition*, pages 4974–4984, 2022. [i](#), [ii](#), [vii](#)
- [45] Zhuofan Xia, Dongchen Han, Yizeng Han, Xuran Pan, Shiji Song, and Gao Huang. Gsva: Generalized segmentation via multimodal large language models. In *Proceedings of the IEEE/CVF Conference on Computer Vision and Pattern Recognition*, pages 3858–3869, 2024. [ii](#)
- [46] Ning Xu, Linjie Yang, Yuchen Fan, Dingcheng Yue, Yuchen Liang, Jianchao Yang, and Thomas Huang. Youtube-vos: A large-scale video object segmentation benchmark. *arXiv preprint arXiv:1809.03327*, 2018. [v](#)

- [47] Shilin Yan, Renrui Zhang, Ziyu Guo, Wenchao Chen, Wei Zhang, Hongyang Li, Yu Qiao, Hao Dong, Zhongjiang He, and Peng Gao. Referred by multi-modality: A unified temporal transformer for video object segmentation. In *Proceedings of the AAAI Conference on Artificial Intelligence*, pages 6449–6457, 2024. [v](#), [vii](#)
- [48] Zhao Yang, Jiaqi Wang, Yansong Tang, Kai Chen, Hengshuang Zhao, and Philip HS Torr. Lavt: Language-aware vision transformer for referring image segmentation. In *Proceedings of the IEEE/CVF Conference on Computer Vision and Pattern Recognition*, pages 18155–18165, 2022. [ii](#)
- [49] Licheng Yu, Patrick Poirson, Shan Yang, Alexander C Berg, and Tamara L Berg. Modeling context in referring expressions. In *Computer Vision–ECCV 2016: 14th European Conference, Amsterdam, The Netherlands, October 11–14, 2016, Proceedings, Part II 14*, pages 69–85. Springer, 2016. [v](#)
- [50] Linfeng Yuan, Miaoqing Shi, Zijie Yue, and Qijun Chen. Losh: Long-short text joint prediction network for referring video object segmentation. In *Proceedings of the IEEE/CVF Conference on Computer Vision and Pattern Recognition*, pages 14001–14010, 2024. [i](#), [ii](#), [vii](#)
- [51] Yuxuan Zhang, Tianheng Cheng, Rui Hu, Lei Liu, Heng Liu, Longjin Ran, Xiaoxin Chen, Wenyu Liu, and Xinggang Wang. Evf-sam: Early vision-language fusion for text-prompted segment anything model. *arXiv preprint arXiv:2406.20076*, 2024. [ii](#), [iii](#), [v](#)
- [52] Bolei Zhou, Hang Zhao, Xavier Puig, Sanja Fidler, Adela Barriuso, and Antonio Torralba. Scene parsing through ade20k dataset. In *Proceedings of the IEEE conference on computer vision and pattern recognition*, pages 633–641, 2017. [v](#)
- [53] Tianfei Zhou, Shunzhou Wang, Yi Zhou, Yazhou Yao, Jianwu Li, and Ling Shao. Motion-attentive transition for zero-shot video object segmentation. In *Proceedings of the AAAI conference on artificial intelligence*, pages 13066–13073, 2020. [i](#)
- [54] Zixin Zhu, Xuelu Feng, Dongdong Chen, Junsong Yuan, Chunming Qiao, and Gang Hua. Exploring pre-trained text-to-video diffusion models for referring video object segmentation. In *European Conference on Computer Vision*, pages 452–469. Springer, 2024. [ii](#), [vii](#)